tvst

https://doi.org/10.1167/tvst.8.6.5

Article

Impact of Bleaching on Photoreceptors in Different Intermediate AMD Phenotypes

Enrico Borrelli[1], Eliana Costanzo[2], Mariacristina Parravano[2], Pasquale Viggiano[3], Monica Varano[2], Paola Giorno[2], Alessandro Marchese[1], Riccardo Sacconi[1], Leonardo Mastropasqua[3], Francesco Bandello[1], and Giuseppe Querques[1]

[1] Ophthalmology Department, San Raffaele University Hospital, Milan, Italy
[2] IRCCS - Fondazione Bietti, Rome, Italy
[3] Ophthalmology Clinic, Department of Medicine and Science of Ageing, University G. D'Annunzio Chieti-Pescara, Chieti, Italy

Correspondence: Giuseppe Querques, Department of Ophthalmology, University Vita-Salute San Raffaele, Via Olgettina 60, Milan, Italy. e-mail: giuseppe.querques@hotmail.it

Received: 18 April 2019
Accepted: 10 September 2019
Published: 12 November 2019

Keywords: age-related macular degeneration; optical coherence tomography; photoreceptors

Citation: Borrelli E, Costanzo E, Parravano M, Viggiano P, Varano M, Giorno P, Marchese A, Sacconi R, Mastropasqua L, Bandello F, Querques G. Impact of bleaching on photoreceptors in different intermediate AMD phenotypes. Trans Vis Sci Tech. 2019;8(6):5, https://doi.org/10.1167/tvst.8.6.5

Purpose: To investigate photoreceptors' structural changes after photobleaching exposure in intermediate age-related macular degeneration (iAMD) eyes with and without reticular pseudodrusen (RPD).

Methods: In this prospective, cross-sectional study, were enrolled iAMD patients and healthy controls. Patients and controls underwent repeated imaging with spectral-domain optical coherence tomography (SD-OCT), at baseline and at three intervals after bleaching, during the subsequent recovery in darkness. Structural changes in photoreceptors were investigated in the foveal region and in four perifoveal areas.

Results: Twenty eyes of 20 iAMD patients (12 with RPD and 8 without RPD) and 15 age-matched healthy controls were enrolled. At baseline, the photoreceptor outer segment (OS) volume was significantly reduced in iAMD eyes with RPD compared with controls, in the foveal and perifoveal regions. In healthy subjects, a precocious increase in OS volume was observed after bleaching in the foveal region, and a rapid recovery to baseline values was recorded. In the perifoveal regions, an increase in OS volume was observed 10 minutes after light onset. In contrast, in iAMD subjects with RPD an altered response to photobleaching, in the foveal and superior and inferior perifoveal regions, was recorded.

Conclusions: Our imaging evidences support the hypothesis that dark adaptation is more altered in eyes with RPD. The structural modifications may explain the functional increased damage of the retinal pigment epithelium and photoreceptors reported in eyes with RPD.

Translational Relevance: OCT imaging may be used to assess dark adaptation in AMD eyes.

Introduction

Age-related macular degeneration (AMD) is the leading cause of irreversible central vision loss among older individuals in developed countries.[1] Intermediate AMD (iAMD) is clinically characterized by the accumulation of drusen and can progress to the late form of AMD notable for choroidal (Types 1 and 2) or retinal neovascularization (Type 3), or geographic atrophy (GA). Reticular pseudodrusen (RPD) represent a distinct AMD phenotype associated with an overall higher incidence of progression to both forms of late AMD.[1]

RPD were first described by Mimoun et al.[2] in 1990 as a peculiar yellowish pattern in the macula, more visible using blue light. A few years later, Arnold and colleagues[3] described histopathologic abnormalities of one eye with RPD and no evidence of drusen, and speculated that RPD may be associated with a loss of choroidal vessels with consequent fibrous replacement of the choroidal stroma. Thereafter, several important studies adopting choroidal imaging have provided evidence that

fibrotic replacement results in a widespread reduction in choroidal thickness[4–8] and choriocapillaris perfusion,[9,10] even in comparison with other AMD phenotypes. Importantly, while RPD are commonly found in AMD eyes, these alterations have also been described in other retinal disorders, including adult-onset foveomacular vitelliform dystrophy (AOFVD).[11] The association between RPD and AOFVD may thus suggest that RPD development is related to retinal pigment epithelium (RPE) dysfunction and consequent impairment in photoreceptor outer segment (OS) turnover.[11,12] Based on these observations arising from integrated imaging, it has been proposed that, in eyes with RPD, fibrosis of the choroid could lead to the derangement of the RPE and secondary accumulation of photoreceptor OS above the RPE.[13]

Although RPD and drusen share some histopathologic similarities and frequently coexist, these two pathologic deposits are extremely different in composition and clinical characteristics. As an example, RPD and drusen have different ultrastructural characteristics, assuming that a higher concentration of unesterified cholesterol, vitronectin, and photoreceptor pigments (including precursors of A2E/lipofuscin) was disclosed in RPD deposits.[14,15] Furthermore, while drusen are mainly confined to the central macula,[16] RPD preferentially localize in the outer macula and/or near-mid retinal periphery.[3] In addition, the functional status of the macula in iAMD eyes is closely associated with the presence of RPD. Compared with drusen, RPD are indeed associated with a more pronounced impairment in macular sensitivity.[17] Dark adaptation may be defined as the delayed recovery of light sensitivity in darkness following prior light exposure (photobleaching). Dark adaption is impaired in iAMD eyes and it was demonstrated that this damage is more evident in eyes with RPD compared with eyes without RPD. This aspect likely reflects a greater dysfunction of the unit comprising RPE and photoreceptors in RPD eyes.[18]

Previous important imaging studies have proved that photobleaching exposure may be associated with significant changes. In detail, fundus autofluorescence studies demonstrated that photobleaching may cause an immediate reduction in signal intensity.[19–22] In addition, previous important studies employing autofluorescence also assessed diseased eyes, which further improve our understanding on this phenomenon.[23,24] Moreover, previous reports employing optical coherence tomography (OCT) have proved that photobleaching exposure, and the subsequent recovery in darkness, is associated with distinctive changes in the length of photoreceptor OS.[25–28]

In the present prospective, cross-sectional study, we investigated photoreceptors' structural changes after photobleaching exposure and during the subsequent recovery in darkness, in iAMD eyes, with or without RPD. Notably, these measurements were determined in different retinal regions in order to provide a topographic analysis of these changes. Our aim was to help shed further light on the relationship between RPD and macular function in iAMD patients. This could be helpful to better understand the disease pathophysiology, and to identify potential biomarkers for disease progression and new targets for pharmacologic treatment.

Methods

Study Participants

This was a prospective observational case series that adhered to the tenets of the Declaration of Helsinki. Institutional review board approval (reference number RET-10-2018) was obtained from IRCCS - Fondazione Bietti, Rome, Italy. Informed consent was obtained from all individual participants included in the study.

All patients were consecutively enrolled at IRCCS - Fondazione Bietti, Rome, Italy, between March and June 2018 and received a complete ophthalmologic examination, which included the measurement of best-corrected visual acuity (BCVA), intraocular pressure (IOP), and dilated ophthalmoscopy.

The inclusion criteria for iAMD eyes included drusen more than 125 μm in diameter with or without pigmentary abnormalities as determined by the retinal physician during clinical examination and confirmed by dense volume OCT (pigment abnormalities on OCT manifesting as intraretinal hyperreflective foci).[29] Exclusion criteria for iAMD eyes were as follows: (1) previous ocular surgery or history of antivascular endothelial growth factor (VEGF) therapy; (2) myopia greater than −6.00 diopters; and (3) any maculopathy secondary to causes other than AMD (including presence of vitreomacular traction syndrome or an epiretinal membrane). The iAMD study cohort was divided into two subgroups according to the presence of RPD, which were identified on infrared reflectance (IR) and OCT images.

Because age may influence quantitative retinal measurements and dark adaption has been demon-

strated to be dependent on age,[30] a control group similar with respect to age and sex was also included in the current analysis.

All control subjects and patients failed to demonstrate evidence of ocular disease or media opacity as evaluated by dilated fundus examination and OCT analysis. Of note, assuming that a cataract may reduce the amount of light that reaches the retina, and thus affect the photobleaching, we did not include patients with a cataract greater than Lens Opacities Classification System (LOCS) grade 3.[31]

Imaging Protocol

Patients underwent spectral-domain (SD)-OCT imaging using the Heidelberg Spectralis device (Heidelberg Engineering, Heidelberg, Germany) with high-resolution (HR) mode, which may obtain OCT scans with an axial resolution of 7 μm in tissue, and a lateral resolution at the retinal surface estimated at approximately 5 μm. Each set of SD-OCT scans consisted of 19 B-scans, each of which comprised 24 averaged scans, covering approximately 5.5 × 4.5-mm area centered on the fovea. To be included in the analysis, a signal strength of at least 25 was required (the manufacturer manual recommended 15 as the borderline quality score).[32]

A previously reported protocol[28] was slightly modified and adopted. Prior to imaging, the study eye was dilated with 1% tropicamide and there were no restrictions on light exposure before arrival in the imaging suite. Imaging was performed in a dark and windowless room, and stray light from electronic equipment was masked. All imaging was performed between 10 AM and 7 PM.

Prior to bleaching, a baseline OCT scan was obtained in darkness. Photobleaching was obtained with a 488-nm wavelength light for 30 seconds, which causes an almost complete cone and rod pigment bleach (~97% and ~96% for cones and rods, respectively).[27,33,34] Of note, although a sustained photopigment bleaching, and hence overaccumulation of retinoids may be harmful, a single complete bleach resulting in a flood of retinoids does not cause light damage.[19] In addition, we used excitation energies that are well below the maximum laser retinal irradiance limits established by the American National Standards Institute and other international standards.[35] Therefore, our protocol may be considered as safe. During photobleaching, subjects were asked to keep their eyes open and look at the internal fixation point. After the bleach, OCT volumes were acquired at 30 seconds, 5 minutes, and 10 minutes, respectively. Assuming that the internal fixation target may cause photobleaching,[36] this was turned off during the follow-up OCT examinations.

OCT Analysis

The OCT images were exported and then imported into image analysis ImageJ software version 1.50 (National Institutes of Health, Bethesda, MD; available at http://rsb.info.nih.gov/ij/index.html). Then, an experienced certified grader (EB) delineated the ellipsoid zone (EZ) and OS surfaces in all the tested regions of interest within macular OCT scans. The EZ was defined as the reflective layer situated posterior to the external limiting membrane (ELM) and anterior to the strong-reflecting interdigitation zone (IZ). The OS was defined as the weak-reflecting layer in between the EZ and IZ. Grading results were exported as binarized images in which thee graded area was white, while the remaining image was black, and automatically calculated in mm^2.

Notably, OCT analysis was performed in five square regions of interest with dimensions of 0.75 × 0.75 mm. The foveal region was centered on the fovea. The perifoveal regions (superior – S, nasal – N, inferior – I, and temporal – T) were placed at 1.0 mm from the foveal region (Figure 1).

Each region of interest comprised three consecutive horizontal OCT B-scans. Assuming that we assessed 5 different macular regions (1 foveal and 4 perifoveal areas) for each patient we graded 15 B-scans at each time points. For each B-scan, we graded the EZ area (EZ_n) and the OS area (OS_n). The photoreceptor EZ and OS volumes were thus calculated using the following formulas:

$$\text{EZ volume} = \frac{(EZ_1 + EZ_2 + EZ_3)}{3} \times W \qquad (1)$$

$$\text{OS volume} = \frac{(OS_1 + OS_2 + OS_3)}{3} \times W \qquad (2)$$

where EZ_n and OS_n represent the graded EZ and OS areas in the three consecutive B-scan images of the considered region, and W is the retinal width occupied by three consecutive B-scans (Fig. 1).

Statistical Analysis

To detect departures from normality distribution, a Shapiro-Wilk's test was performed for all variables. Means and standard deviation (SD) were computed for all quantitative variables. Continuous variables at baseline were compared by conducting a one-way

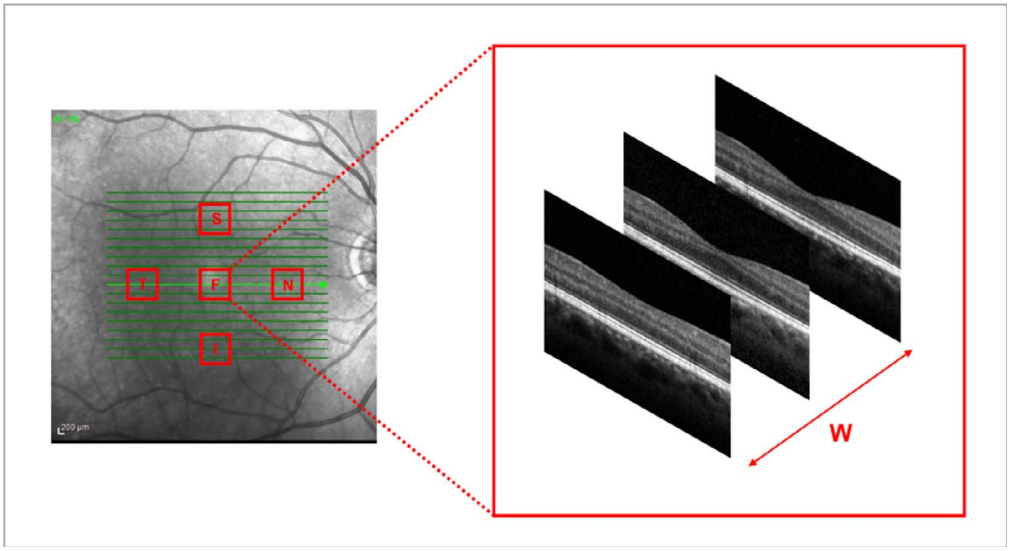

Figure 1. Representation of the regions of interest used to investigate photoreceptor volume changes. OCT variables were investigated in five square regions of interest with dimension of 0.75 × 0.75 mm. The foveal region was centered on the fovea. The perifoveal regions (superior – S, nasal – N, inferior – I, and temporal – T) were placed at 1.0 mm from the foveal region. Each region of interest comprised three consecutive horizontal OCT B-scans. Photoreceptor EZ and OS volumes were thus investigated using formulas, which take into account the width (W) occupied by three consecutive B-scans.

analysis of variance (ANOVA) analysis with Bonferroni post-hoc test. Paired-samples *t*-test was conducted to investigate differences in continuous variables between follow-up and baseline values within the three groups. The two-way mixed, average measure intraclass correlation coefficient (ICC) was calculated on 10 randomly selected eyes (5 healthy and 5 iAMD eyes), which were graded by two graders, in order to assess interobserver variation in assessing EZ and OS volume assessment.

Statistical calculations were performed using Statistical Package for Social Sciences (version 20.0; SPSS Inc., Chicago, IL). The chosen level of statistical significance was $P < 0.05$.

Results

Characteristics of Patients Included in the Analysis

Of 35 patients included in this analysis, 20 (13 female) were diagnosed with iAMD and 15 (11 female) were healthy controls. The iAMD cohort was divided into two subgroups according to the presence of RPD, yielding a group of 12 cases with RPD (iAMD with RPD group), and eight cases without RPD (iAMD without RPD group) (Table 1).

Mean ± SD age was 73.9 ± 11.0 years (range, 53–85 years) in the control group, 75.9 ± 7.1 years (range, 61–86 years) in the iAMD without RPD group, and 77.0 ± 8.2 years (range, 64–88 years) in the iAMD with RPD group ($P > 0.05$ in all the comparisons) (Table 1).

Photoreceptor OCT Measurements at Baseline

At baseline, the OS volume was significantly reduced in iAMD eyes with RPD compared with control eyes, in the foveal and perifoveal regions (Table 2). In the iAMD without RPD group, the OS volume was slightly lower numerically at baseline, as compared with the control group, although this difference did not reach the statistical significance in the perifoveal regions (Table 2).

The EZ volume did not significantly differ among the three groups (Table 2).

Photoreceptor OCT Measurements After Bleaching

The time course of photoreceptor EZ and OS volume changes relative to baseline was determined within the three groups (Tables 3 and 4, Figs. 2 and 3).

In healthy subjects, an increase in OS volume was observed 30 seconds after bleaching in the foveal region, and a recovery to baseline occurred at the next two timepoints, 5 and 10 minutes after the bleach. In

Table 1. Characteristics of AMD Patients and Controls

	Healthy Controls	Intermediate AMD Without RPD	Intermediate AMD With RPD
Number of eyes enrolled (patients)	15 (15)	8 (8)	12 (12)
Age, y	73.9 ± 11.0	75.9 ± 7.1	77.0 ± 8.2
Sex	11 F	5 F	8 F
BCVA, Snellen equivalent	20/20	20/20	20/20

RPD, reticular pseudodrusen.

Table 2. Baseline Values of Photoreceptor Volumes in Patients and Controls

	Group		
OS Volume, mm^3	Healthy Controls	Intermediate AMD Without RPD	Intermediate AMD With RPD
F	0.173 ± 0.021	0.142 ± 0.032 **0.023**[a]	0.108 ± 0.022 **<0.0001**[a] 0.434[b]
N	0.151 ± 0.034	0.135 ± 0.036 0.675[a]	0.120 ± 0.019 **0.039**[a] 0.969[b]
T	0.152 ± 0.026	0.143 ± 0.035 1.0[a]	0.120 ± 0.020 **0.033**[a] 0.424[b]
S	0.151 ± 0.027	0.135 ± 0.026 0.632[a]	0.098 ± 0.029 **<0.0001**[a] **0.014**[b]
I	0.147 ± 0.022	0.135 ± 0.029 0.932[a]	0.099 ± 0.029 **<0.0001**[a] **0.014**[b]
EZ Volume, mm^3			
F	0.122 ± 0.015	0.124 ± 0.013 0.864[a]	0.126 ± 0.016 0.561[a] 0.771[b]
N	0.117 ± 0.013	0.108 ± 0.011 0.440[a]	0.103 ± 0.016 0.071[a] 1.0[b]
T	0.120 ± 0.012	0.114 ± 0.013 0.957[a]	0.106 ± 0.017 0.095[a] 0.616[b]
S	0.102 ± 0.019	0.112 ± 0.011 0.466[a]	0.098 ± 0.012 1.0[a] 0.144[b]
I	0.103 ± 0.018	0.114 ± 0.011 0.317[a]	0.099 ± 0.012 1.0[a] 0.067[b]

[a] Comparison versus "healthy controls."
[b] Comparison versus "iAMD w/o RPD."

Values were compared by one-way analysis of variance (ANOVA), followed by Bonferroni post hoc test. Significant *P* values are in bold. AMD, age-related macular degeneration; RPD, reticular pseudodrusen; OS, photoreceptor outer segment; EZ, photoreceptor ellipsoid zone.

Table 3. Photoreceptor Outer Segment Volume in Patients and Controls

Group	Region	OS Volume, mm^3			
		Baseline	30 s	5 min	10 min
Healthy controls	F	0.173 ± 0.021	0.179 ± 0.029*	0.170 ± 0.033	0.167 ± 0.028*
	N	0.151 ± 0.034	0.153 ± 0.033	0.156 ± 0.035	0.156 ± 0.036
	T	0.152 ± 0.026	0.157 ± 0.026	0.158 ± 0.034	0.158 ± 0.029*
	S	0.151 ± 0.027	0.151 ± 0.024	0.151 ± 0.031	0.160 ± 0.024*
	I	0.147 ± 0.022	0.148 ± 0.020	0.148 ± 0.031	0.156 ± 0.025*
Intermediate AMD without RPD	F	0.142 ± 0.032	0.172 ± 0.030*	0.136 ± 0.019	0.137 ± 0.026
	N	0.135 ± 0.036	0.141 ± 0.029	0.136 ± 0.019	0.145 ± 0.024*
	T	0.143 ± 0.035	0.143 ± 0.030	0.146 ± 0.022	0.147 ± 0.022
	S	0.135 ± 0.026	0.131 ± 0.013	0.148 ± 0.033	0.163 ± 0.030*
	I	0.135 ± 0.029	0.133 ± 0.017	0.152 ± 0.038	0.160 ± 0.033*
Intermediate AMD with RPD	F	0.108 ± 0.022	0.116 ± 0.025*	0.127 ± 0.020*	0.128 ± 0.036*
	N	0.120 ± 0.019	0.121 ± 0.023	0.121 ± 0.024	0.127 ± 0.017*
	T	0.120 ± 0.020	0.120 ± 0.024	0.118 ± 0.025	0.130 ± 0.018*
	S	0.098 ± 0.029	0.120 ± 0.033*	0.114 ± 0.037*	0.113 ± 0.042*
	I	0.099 ± 0.029	0.121 ± 0.033*	0.115 ± 0.033*	0.114 ± 0.042*

* $P < 0.05$ in the comparison with baseline values using paired-samples *t*-test.

the perifoveal regions, there was no change at 30 seconds and 5 minutes after the bleach, but an increase in OS volume was observed 10 minutes after bleaching; this difference did not reach the statistical significance in the nasal field.

In similarity with healthy controls, the foveal region in the iAMD without RPD group was characterized by a significant increase in OS volume 30 seconds after bleaching. Furthermore, the parafoveal regions displayed an expansion in OS volume 10 minutes after the bleach (this difference did not reach the statistical significance in the temporal field).

In contrast, subjects with iAMD and RPD were characterized by an altered response to photobleach-

Table 4. Ellipsoid Zone Volume in Patients and Controls

Group	Region	EZ Volume, mm^3			
		Baseline	30 s	5 min	10 min
Healthy controls	F	0.122 ± 0.015	0.122 ± 0.021	0.121 ± 0.012	0.122 ± 0.011
	N	0.117 ± 0.013	0.113 ± 0.010	0.114 ± 0.017	0.112 ± 0.013
	T	0.120 ± 0.012	0.119 ± 0.014	0.116 ± 0.014	0.115 ± 0.015
	S	0.102 ± 0.019	0.103 ± 0.012	0.100 ± 0.019	0.100 ± 0.013
	I	0.103 ± 0.018	0.104 ± 0.011	0.102 ± 0.021	0.104 ± 0.012
Intermediate AMD without RPD	F	0.124 ± 0.013	0.123 ± 0.010	0.122 ± 0.013	0.124 ± 0.019
	N	0.108 ± 0.011	0.108 ± 0.009	0.114 ± 0.011	0.112 ± 0.008
	T	0.114 ± 0.013	0.111 ± 0.010	0.116 ± 0.009	0.112 ± 0.011
	S	0.112 ± 0.011	0.114 ± 0.010	0.113 ± 0.012	0.109 ± 0.012
	I	0.114 ± 0.011	0.114 ± 0.009	0.113 ± 0.011	0.111 ± 0.009
Intermediate AMD with RPD	F	0.126 ± 0.016	0.125 ± 0.022	0.124 ± 0.013	0.124 ± 0.015
	N	0.103 ± 0.016	0.105 ± 0.014	0.104 ± 0.009	0.108 ± 0.010
	T	0.106 ± 0.017	0.108 ± 0.014	0.107 ± 0.009	0.111 ± 0.009
	S	0.098 ± 0.012	0.107 ± 0.012	0.110 ± 0.011	0.109 ± 0.010
	I	0.099 ± 0.012	0.108 ± 0.012	0.111 ± 0.011	0.109 ± 0.010

$P > 0.05$ in all the comparisons between baseline and follow-up values using paired-samples *t*-test.

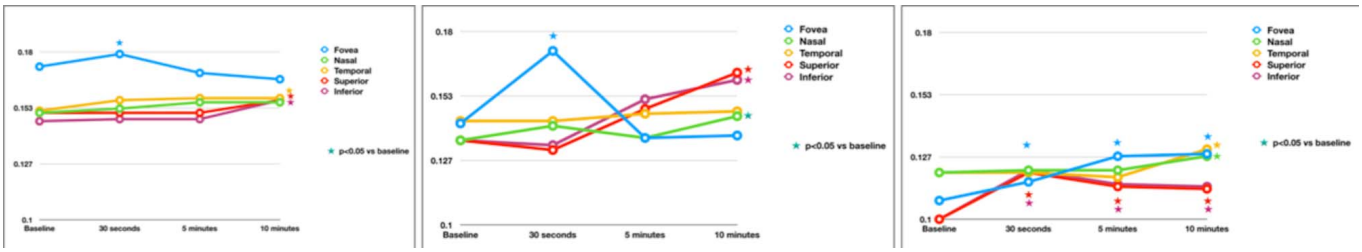

Figure 2. Photoreceptor OS volume changes after bleaching and during following recovery. Curves of the photoresponses from healthy controls (*left*), iAMD eyes without RPD (*middle*), and iAMD eyes with RPD (*right*). *Empty circles* represent mean values. Significant changes compared with baseline values are marked with *colored stars*. Standard deviation values are presented in Table 2.

ing in the foveal and superior and inferior perifoveal regions. These regions had a significant rapid and longstanding increase in OS volume. Differently, the nasal and temporal perifoveal regions exhibited a significant expansion in OS volume only 10 minutes after the bleach, these two regions thus reproducing responses similar to healthy subjects.

The EZ volume did not exhibit significant changes throughout the examinations, in both patients and healthy controls (Table 4).

Interobserver Agreement

Agreement was found to be excellent in the EZ and OS volume assessment (ICC = 0.911 and ICC = 0.925, respectively).

Discussion

In this cross-sectional study, we prospectively investigated photoreceptor structural modifications occurring after photobleaching exposure and during the subsequent recovery in darkness, in iAMD eyes, with or without RPD. Overall, we observed that iAMD eyes with RPD are characterized by significant alterations in the OS photoreceptor responses to bleaching. In contrast to previous studies,[26,27] we employed a commercially available OCT device. Therefore, future studies will be allowed to validate our results and these findings might become an imaging biomarker of functional dark adaptation.

Data from a number of studies using distinct approaches indicated that photoreceptor OS elongation occurs as a physiologic response to bleaching. Li et al.[25] reported a light-stimulated increase in the OS thickness in mice using an ultra-high resolution (UHR)-OCT system. They also directly confirmed with histology that this imaging-detected elongation corresponded to an increase in length of photoreceptor OS. These conclusions in mice were further validated in the Zhang and colleagues' study.[26] Lu and colleagues[27] were first to confirm these findings in healthy humans. They imaged five healthy eyes (5 subjects, ages 26–35 years) with UHR-OCT and demonstrated an OS lengthening following strong light exposure, and recovery during subsequent dark adaptation. Importantly, cone and rod cells displayed significant differences in this physiologic response: while cone OS thickens rapidly after the bleach, followed by a rapid decline to baseline values, which are reached in less than 5 minutes, the rod photoresponses require 5 to 7 minutes to reach their maxima, and then recover to baseline over times ranging from 15 to 30 minutes.[27] Our results confirm these prior reports in animals and humans of OS enlargement following strong light exposure, and recovery during subsequent dark adaptation. Importantly, we first show these dynamic changes in an elderly healthy cohort (ages 60–85). In addition, we provided a topographic analysis of these physiologic changes and exhibited that in the foveal region, where cone density is greatest, the increase in OS volume and recovery are fast, while in the perifoveal regions, where rod density is higher, photoreceptor OS volume needs as long as 10 minutes to be significantly increase.

The mechanism(s) driving photoreceptor OS elongation after bleaching have been debated. It has been hypothesized that OS thickening represents an osmotic swelling response to an increase in OS osmolarity triggered by phototransduction.[26,27]

A previous adaptive optics (AO)-OCT imaging study of cone photoreceptors in humans demonstrated shortening of cone OS, which was independent on bleaching stimulation.[37] This change in OS thickness, which resulted opposite in sign to the bleach-dependent increased volume we observed, was interpreted to be secondary to disk shedding, which consists in the RPE cell phagocytosis of the OS. Disk shedding is known to be linked to a circadian cycle

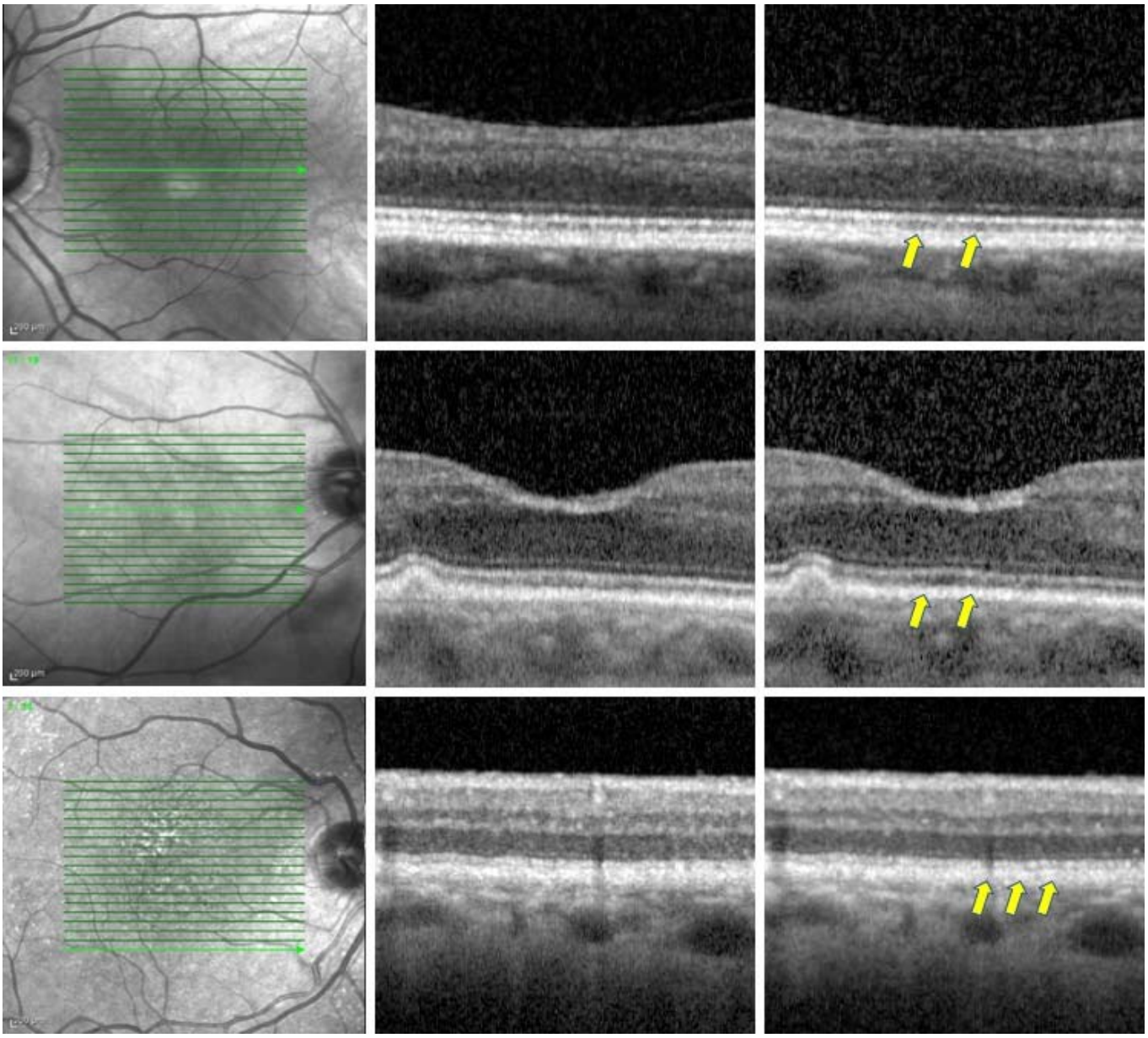

Figure 3. Representation of healthy and AMD cases. Representative OCT images from a healthy subject (*above*) and two AMD patients, without (*middle row*) and with RPD (*bottom row*), respectively. The *green arrow* on the near-infrared reflectance images (*left*) shows the location and direction of the structural OCT B-scans. Thirty seconds after bleaching (*right images*), an elongation of the photoreceptor OS was noted (highlighted with *yellow arrows* in the figure), compared with the correspondent baseline structural OCT B-scans (*middle images*).

and most actively occurs in the early morning.[37–41] For this reason, our study cohort underwent imaging in the late morning to afternoon, in order to avoid this process from confounding the analysis.

We add to the literature by reporting photoreceptor structural modifications occurring after the bleach and during the following recovery in darkness, in iAMD eyes. One of the most notable observations from our study was that, whereas iAMD eyes without RPD do not show significant alterations in this physiologic response, iAMD eyes with RPD have significant alterations in the OS photoreceptor response to bleaching.

In details, eyes with RPD displayed an early and longstanding photoreceptor OS enlargement following light exposure, without a significant recovery in the examined 10 minutes after bleaching, in both the foveal and perifoveal regions, these findings

corroborating the hypothesis that cone and rod cells are both impaired in RPD eyes. Indeed, although RPD are known to have a predilection for rod-dominated areas of the retina, as nicely displayed by both imaging and microperimetry studies,[13,42] cones were demonstrated to be significantly affected in RPD eyes.[43] Importantly, within the perifoveal region, we displayed that these alterations have regional differences, assumed that exclusively the superior and inferior areas exhibited these changes. Our imaging data are thus in agreement with previous evidences showing that the formation of RPD within the perifovea is not spatially random but may predilect the superior and inferior regions.[3,7,44]

The significant early and longstanding photoreceptor OS enlargement following light exposure in RPD eyes would be consistent with photoreceptor dysfunction. Therefore, this may impair translocation of phototransduction components out of the OS, which protects photoreceptors from osmotic stress.[26] Several theories have been proposed to explain photoreceptor impairment in RPD eyes, including a direct mechanical compression of RPD on photoreceptors, which may provide a physical impediment to transport out of the OS. Our results seem to corroborate this hypothesis, taking into account that the OS volume was significantly reduced at baseline in the iAMD with RPD group. Alternatively, choroidal hypoperfusion among RPD eyes could represent another mechanism for photoreceptor damage and decreased retinoid availability. A third possibility is that photoreceptor dysfunction may be actually secondary to an abnormality of the retinoid cycle at the level of RPE; thus, an impediment in regeneration of 11-cis retinal by the RPE could affect the functional state of photoreceptors. In support to the latter hypothesis, there are histopathologic evidences showing that RPD can supplant RPE cells, instead of just overlying them, in certain instances.[44] Furthermore, similar to vitelliform lesions, RPD were demonstrated to be composed of lipofuscin-like material representing unphagocytized photoreceptor OS, which may be interpreted as an indirect sign of RPE dysfunction.[12] In addition, in similarity to our findings in RPD eyes, Abràmoff et al.[28] have recently demonstrated that eyes with Best disease, which is known to be caused by RPE impairment, are characterized by a longstanding photoreceptor OS enlargement following light exposure.

Our study has limitations, including the cross-sectional nature of the study. A prospective longitudinal evaluation of photobleaching in healthy and iAMD subjects may allow to recognize potential biomarkers for disease development or progression. Furthermore, although we adopted high-resolution OCT with eye-tracking technology, fluctuations in the measurements may have limited the ability to detect some of these responses. For example, some variation may arise from cell-to-cell length differences, from speckle noise in the OCT, or from inaccuracy in eye tracking. To limit these fluctuations, we felt the safest strategy was to investigate changes in photoreceptor volume rather than thickness, this representing an averaged assessment in three consecutive scans. Another limitation of this study is that the outer retinal layers become disrupted in outer retinal disease, and therefore the individual EZ and interdigitation layer lines are more difficult to visualize and therefore more difficult to delineate. However, our study was not designed to compare healthy and pathological eyes, but rather to investigate changes after bleaching within groups and compare these changes. Moreover, media opacities may impact on the amount of light reaching the retina and thus on the photobleaching. Even though we excluded patients with media opacities (e.g., cataract greater than LOCS grade 3), we are not sure that tiny changes in media clarity may have not influenced—even partially—our results. A final limitation is that the testing protocol used in this study was limited to 10 minutes after bleaching, which we estimated to be a reasonable testing time for an elderly population. However, this did not allow us to fully investigate the recovery period during dark adaption, especially in the perifoveal regions.

In summary, in this OCT study we have measured reliable, localized changes in the human photoreceptor bands after flash exposure and subsequent dark adaptation. These structural modifications might be considered as an imaging surrogate for functional dark adaptation. Our results provide imaging evidence to support the hypothesis that dark adaptation is more altered in eyes with RPD and this may shed light on structural and functional consequences correlated to an increased damage of the RPE and photoreceptors in RPD eyes. Assuming that dark adaptation is a very complex process with very well-known kinetics, future studies will be required to confirm our results and straighten our conclusions.

Acknowledgments

Supported by grants from the Italian Ministry of Health and Fondazione Roma.

Disclosure: **E. Borrelli**, None; **E. Costanzo**, None; **M. Parravano**, Allergan (S), Bayer (S), Novartis (S); **P. Viggiano**, None; **M. Varano**, None; **P. Giorno**, None; **A. Marchese**, None; **R. Sacconi**, None; **L. Mastropasqua**, None; **F. Bandello**, Allergan (S), Alimera (S), Bayer (S), Farmila-Thea (S), Schering Pharma (S), Sanofi-Aventis (S), Novagali (S), Pharma (S), Hoffmann-La Roche (S), Genetech (S), Novartis (S); **G. Querques**, Allergan (S), Alimera (S), Amgen (S), Bayer (S), Khb (S), Novartis (S), Roche (S), Sandoz (S), Zeiss (S), Allergan (C), Alimera (C), Bausch And Lomb (C), Bayer (C), Heidelberg (C), Novartis (C), Zeiss (C)

References

1. Friedman DS, O'Colmain BJ, Muñoz B, et al. Prevalence of age-related macular degeneration in the United States. *Arch Ophthalmol*. 2004;122(4): 564–572.
2. Mimoun G, Soubrane G, Coscas G. Les drusen maculaires [in French]. *J Fr Ophtalmol*. 1990;13: 511–530.
3. Arnold JJ, Sarks SH, Killingsworth MC, Sarks JP. Reticular pseudodrusen: a risk factor in age-related maculopathy. *Retina*. 1995;15:183–191.
4. Corvi F, Souied EH, Capuano V, et al. Choroidal structure in eyes with drusen and reticular pseudodrusen determined by binarisation of optical coherence tomographic images. *Br J Ophthalmol*. 2017;101:348–352.
5. Switzer DW, Mendonça LS, Saito M, Zweifel SA, Spaide RF. Segregation of ophthalmoscopic characteristics according to choroidal thickness in patients with early age-related macular degeneration. *Retina*. 2012;32:1265–1271.
6. Garg A, Oll M, Yzer S, et al. Reticular pseudodrusen in early age-related macular degeneration are associated with choroidal thinning. *Invest Ophthalmol Vis Sci*. 2013;54:7075–7081.
7. Querques G, Querques L, Forte R, Massamba N, Coscas F, Souied EH. Choroidal changes associated with reticular pseudodrusen. *Invest Ophthalmol Vis Sci*. 2012;53:1258–1263.
8. Capuano V, Souied EH, Miere A, Jung C, Costanzo E, Querques G. Choroidal maps in non-exudative age-related macular degeneration. *Br J Ophthalmol*. 2016;100:677–682.
9. Nesper PL, Soetikno BT, Fawzi AA. Choriocapillaris nonperfusion is associated with poor visual acuity in eyes with reticular pseudodrusen. *Am J Ophthalmol*. 2017;174:42–55.
10. Cicinelli MV, Rabiolo A, Marchese A, et al. Choroid morphometric analysis in non-neovascular age-related macular degeneration by means of optical coherence tomography angiography. *Br J Ophthalmol*. January 2017;101:1193–1200.
11. Zweifel SA, Spaide RF, Yannuzzi LA. Acquired vitelliform detachment in patients with subretinal drusenoid deposits (reticular pseudodrusen). *Retina*. 2011;31:229–234.
12. Querques G, Querques L, Martinelli D, et al. Pathologic insights from integrated imaging of reticular pseudodrusen in age-related macular degeneration. *Retina*. 2011;31:518–526.
13. Rabiolo A, Sacconi R, Cicinelli MV, Querques L, Bandello F, Querques G. Spotlight on reticular pseudodrusen. *Clin Ophthalmol*. 2017;11:1707–1718.
14. Curcio CA, Presley JB, Millican CL, Medeiros NE. Basal deposits and drusen in eyes with age-related maculopathy: evidence for solid lipid particles. *Exp Eye Res*. 2005;80:761–775.
15. Greferath U, Guymer RH, Vessey KA, Brassington K, Fletcher EL. Correlation of histologic features with in vivo imaging of reticular pseudodrusen. *Ophthalmology*. 2016;123:1320–1331.
16. Curcio CA. Photoreceptor topography in ageing and age-related maculopathy. *Eye*. 2001;15:376–383.
17. Querques G, Massamba N, Srour M, Boulanger E, Georges A, Souied EH. Impact of reticular pseudodrusen on macular function. *Retina*. 2014; 34:321–329.
18. Flamendorf J, Agrón E, Wong WT, et al. Impairments in dark adaptation are associated with age-related macular degeneration severity and reticular pseudodrusen. *Ophthalmology*. 2015;122:2053–2062.
19. Hunter JJ, Morgan JIW, Merigan WH, Sliney DH, Sparrow JR, Williams DR. The susceptibility of the retina to photochemical damage from visible light. *Prog Retin Eye Res*. 2012;31:28–42.
20. Morgan JIW, Hunter JJ, Merigan WH, Williams DR. The reduction of retinal autofluorescence caused by light exposure. *Invest Ophthalmol Vis Sci*. 2009;50:6015–6022.

21. Morgan JIW, Hunter JJ, Masella B, et al. Light-induced retinal changes observed with high-resolution autofluorescence imaging of the retinal pigment epithelium. *Invest Ophthalmol Vis Sci*. 2008;49:3715–3729.
22. Klemm M, Sauer L, Klee S, et al. Bleaching effects and fluorescence lifetime imaging ophthalmoscopy. *Biomed Opt Express*. 2019;10:1446–1461.
23. Choi KE, Yun C, Kim YH, Kim SW, Oh J, Huh K. The effect of photopigment bleaching on fundus autofluorescence in acute central serous chorioretinopathy. *Retina*. 2017;37:568–577.
24. Joseph A, Rahimy E, Freund KB, Sorenson JA, Sarraf D. Fundus autofluorescence and photoreceptor bleaching in multiple evanescent white dot syndrome. *Ophthalmic Surg Lasers Imaging Retina*. 2013;44:588–592.
25. Li Y, Fariss RN, Qian JW, Cohen ED, Qian H. Light-induced thickening of photoreceptor outer segment layer detected by ultra-high resolution OCT imaging. *Invest Ophthalmol Vis Sci*. 2016;57:OCT105–OCT111.
26. Zhang P, Zawadzki RJ, Goswami M, et al. In vivo optophysiology reveals that G-protein activation triggers osmotic swelling and increased light scattering of rod photoreceptors. *Proc Natl Acad Sci U S A*. 2017;114:E2937–E2946.
27. Lu CD, Lee B, Schottenhamml J, Maier A, Pugh EN, Fujimoto JG. Photoreceptor layer thickness changes during dark adaptation observed with ultrahigh-resolution optical coherence tomography. *Invest Ophthalmol Vis Sci*. 2017;58:4632–4643.
28. Abràmoff MD, Mullins RF, Lee K, et al. Human photoreceptor outer segments shorten during light adaptation. *Invest Ophthalmol Vis Sci*. 2013;54:3721–3728.
29. Ferris FL, Wilkinson CP, Bird A, et al. Clinical classification of age-related macular degeneration. *Ophthalmology*. 2013;120:844–851.
30. Jackson GR, Owsley C, McGwin G. Aging and dark adaptation. *Vision Res*. 1999;39:3975–3982.
31. Chylack LT Jr, Wolfe JK, Singer DM, et al. The Lens Opacities Classification System III. The Longitudinal Study of Cataract Study Group. *Arch Ophthalmol*. 1993;111:831–836.
32. Huang Y, Gangaputra S, Lee KE, et al. Signal quality assessment of retinal optical coherence tomography images. *Invest Ophthalmol Vis Sci*. 2012;53:2133–2141.
33. Paupoo AAV, Mahroo OAR, Friedburg C, Lamb TD. Human cone photoreceptor responses measured by the electoretinogram a-wave during and after exposure to intense illumination. *J Physiol*. 2000;529:469–482.
34. Thomas MM, Lamb TD. Light adaptation and dark adaptation of human rod photoreceptors measured from the a-wave of the electroretinogram. *J Physiol*. 1999;518(Pt 2):479–496.
35. ANSI Z136.1. *American National Standard for the Safe Use of Lasers*. American National Standards Institute; 11 West 42nd Street, New York, New York 10036, USA. 2014;1–258.
36. Tomasso L, Benatti L, Carnevali A, et al. Photobleaching by spectralis fixation target. *JAMA Ophthalmol*. 2016;349:1060–1062.
37. Kocaoglu OP, Liu Z, Zhang F, Kurokawa K, Jonnal RS, Miller DT. Photoreceptor disc shedding in the living human eye. *Biomed Opt Express*. 2016;7:4554.
38. LaVail MM. Rod outer segment disk shedding in rat retina: relationship to cyclic lighting. *Science*. 1976;194:1071.
39. Goldman AI, Teirstein PS, O'Brien PJ. The role of ambient lighting in circadian disc shedding in the rod outer segment of the rat retina. *Invest Ophthalmol Vis Sci*. 1980;19:1257–1267.
40. Goldman AI. The sensitivity of rat rod outer segment disc shedding to light. *Invest Ophthalmol Vis Sci*. 1982;22:695–700.
41. Bobu C, Hicks D. Regulation of retinal photoreceptor phagocytosis in a diurnal mammal by circadian clocks and ambient lighting. *Invest Ophthalmol Vis Sci*. 2009;50:3495–3502.
42. Steinberg JS, Fitzke FW, Fimmers R, Fleckenstein M, Holz FG, Schmitz-Valckenberg S. Scotopic and photopic microperimetry in patients with reticular drusen and age-related macular degeneration. *JAMA Ophthalmol*. 2015;133:690–697.
43. Wu Z, Ayton LN, Makeyeva G, Guymer RH, Luu CD. Impact of reticular pseudodrusen on microperimetry and multifocal electroretinography in intermediate age-related macular degeneration. *Invest Ophthalmol Vis Sci*. 2015;56:2100–2106.
44. Curcio CA, Messinger JD, Sloan KR, Mcgwin G, Medeiros NE, Spaide RF. Subretinal drusenoid deposits in non-neovascular age-related macular degeneration. *Retina*. 2013;33:265–276.